IUST
Iran University of Science and Technology

Iranian Journal of Electrical and Electronic Engineering

Journal Homepage: ijeee.iust.ac.ir

Research Paper

Steady-State Analysis of Hybrid Synchronous Machine With Higher Reluctance to Excitation Power Ratio

E. O. Agbachi*,**, L. U. Anih**(C.A.), and E. S. Obe**

Abstract: The paper presents the steady-state analysis of a new hybrid synchronous machine with a higher reluctance to excitation power ratio. The machine comprises a round rotor and a salient-pole machine elements that are mechanically coupled together and integrally wound. In each stator, there are two sets of identical poly-phase windings identifiable as the primary and secondary windings which are electrically isolated but magnetically coupled. The primary windings are connected in series between the two sections of the hybrid machine while the secondary windings are connected in anti-series and terminated across a balanced capacitor bank. The hybrid machine exhibits a special feature that when running at the synchronous speed, its effective X_D/X_Q ratio can be amplified and hence its output by the tuning of the variable capacitance bank which capacitive reactance X_C neutralizes only the quadrature axis reactance X_Q while the direct axis reactance X_D remains unaffected. It is shown that at X_D/X_Q = 3, the reluctance component of the output power is 2.5 times the excitation power. The calculated and the measured results from the machine are in good conformity.

Keywords: Capacitive Reactance X_C, Primary and Secondary Windings, Variable Capacitor Bank, X_D/X_Q Ratio.

1 Introduction

SYNCHRONOUS reluctance machine is an electrical machine whose torque production utilizes the concept of reluctance and rotating sinusoidal magnetomotive force. This machine has attracted the attention of researchers due to its robustness, low cost as well as high overload capabilities [1-3]. However, the machine has inherent low torque/power density and power factor when compared with permanent magnet synchronous machine or induction machine of the same dimension [4, 5].

Iranian Journal of Electrical and Electronic Engineering, 2022.
Paper first received 03 August 2021, revised 02 October 2021, and accepted 04 October 2021.
* The author is with the Department of Electrical and Electronics Engineering, Federal University of Technology, Minna, Niger State, Nigeria.
E-mail: euokenna@futminna.edu.ng.
** The authors are with the Department of Electrical Engineering, University of Nigeria, Nsukka, Enugu State Nigeria, Nigeria.
E-mails: linus.anih@unn.edu.ng and simon.obe@unn.edu.ng.
Corresponding Author: L. U. Anih.
https://doi.org/10.22068/IJEEE.18.1.2251

There are various studies aimed at improving the output power of the machine through the ingenious design and re-design of the rotor structure [6]–[8]. These attempts have been targeted towards enhancing the saliency ratio (X_d/X_q) of the machine on which the output power depends through the reduction of the q-axis reactance X_q. The problem with this approach is the attendant reduction in the d-axis reactance X_d as well which results in a ratio that is less than the intended value.

Due to the problems associated with the manipulation of rotor geometries to increase the saliency ratio, some researchers undertook investigative studies on capacitor assisted synchronous machines so as to overcome some of the problems. Anih and Agu [9] introduced a novel scheme of increasing the saliency ratio without altering the rotor geometry. This scheme consists of two sets of identical windings on the stator designated as the main and auxiliary windings. The main winding is connected to the mains supply while the auxiliary winding is connected to a balanced capacitor. In this scheme, varying of the capacitance value of the auxiliary winding varies the overall q-axis reactance of the machine. Obe *et al.* [10-12] presented a machine operating on this scheme with improved power factor

and with minimized losses at certain capacitor values.

Anih *et al*. [13, 14] in their recent study investigated that even though varying the capacitor value reduces the q-axis reactance, it also has an attendant deleterious effect on the d-axis reactance. They then introduced a hybrid reluctance machine comprising two machine elements (one round rotor and the other salient-pole rotor) in which the first machine provides only d-axis reactance X_d. By this, the d-axis reactance of the hybrid machine remains constant irrespective of the value of the q-axis reactance. The round rotor half of this hybrid machine has neither field nor damper windings and subsequently does not produce any torque. Its function is merely to produce a synchronous reactance X_S which is made equal to the direct axis reactance X_d of the salient-pole section.

This study is an extension of the work reported in [14], whereby a dc field winding which spans both halves of the hybrid machine is now introduced in the combined rotor and transforms the machine from synchronous reluctance machine to a pure synchronous machine. Also, this hybrid machine will be able to operate as a standalone generator and when operated as a motor, it will be self-starting and self-synchronizing.

3 Description of the Hybrid Machine

The hybrid machine consists of two synchronous machine elements; a salient-pole type mechanically coupled to a round rotor type and each of them has two sets of poly-phase stator windings. One set of the windings is connected in series phase by phase but transposed between the two sections of the machine while the other is connected simply in series phase by phase and identical phases occupy the same slots. Any of the winding sets may be connected to the mains while the other is connected to a variable capacitor bank. The windings connected to the mains will henceforth be referred to as the primary stator winding while that connected across the capacitor bank as the secondary stator winding. A simple dc field winding spans both halves of the machine rotor and also included in the respective rotors are damper windings. The 3-phase and per phase schematic diagrams of the machine are shown in Fig. 1

3 Enhancement of X_D/X_Q Ratio of the Hybrid Machine

The round rotor half of the machine has a constant synchronous reactance X_S while the salient-pole half has two definite axes of geometry, known as the direct and quadrature axes and their associated direct and quadrature axes reactances X_d and X_q respectively.

The synchronous reactance of the round rotor half is made equal to the direct axis reactance X_d of the salient-pole half in magnitude (ie. $X_S = X_d$) by the adjustment of the air-gaps of the round rotor and salient pole halves [15] . When the axis of the salient-pole half coincides with the d-axis, the overall d-axis reactance is $X_D = X_d + X_d = 2X_d$. And when it coincides with the q-axis, the overall q-axis reactance is $X_Q = X_d + X_q$, giving a saliency ratio of $X_D/X_Q = 2X_d/(X_d + X_q) = 2k/(1+k)$, where $k = X_d / X_q$.

The reluctance component of the output power of the hybrid machine is directly proportional to the X_D/X_Q ratio [14, 16]. It is shown in the subsequent subsection of this paper that X_Q is dependent on the negative variable capacitance bank reactance X_C which neutralizes the quadrature axis reactance X_Q as X_C is varied while X_D remains unaffected by the variation. As X_Q tends to zero, X_D/X_Q tends to infinity theoretically [17]. In practice, the machine will be operated at a load angle below the infinite output region for stability consideration.

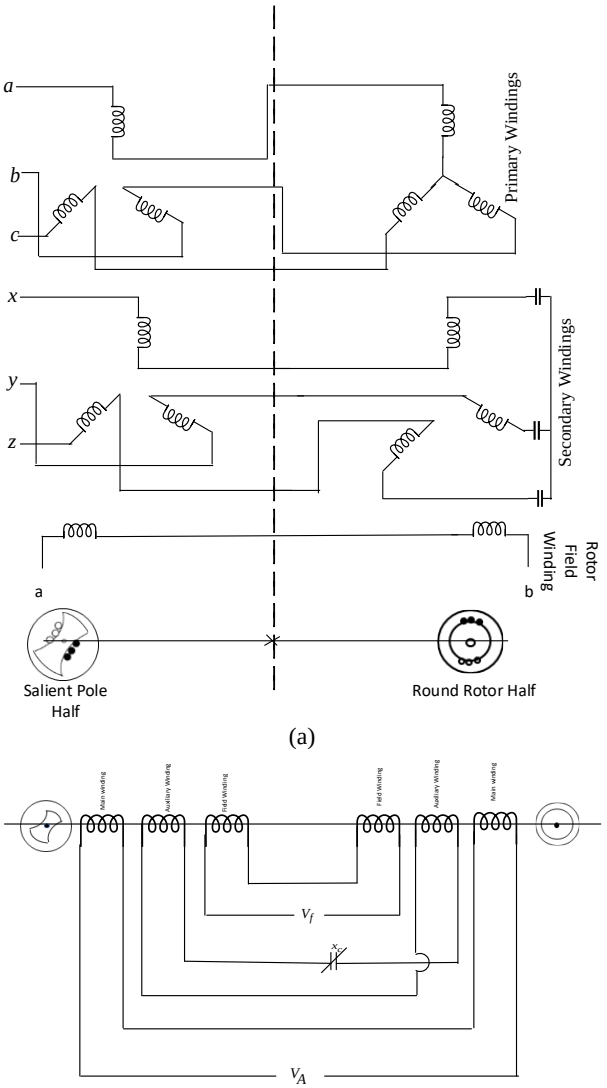

Fig. 1 a) 3-Phase schematic diagram of the hybrid synchronous machine and b) Per-phase schematic diagram of the hybrid machine.

4 Mathematical Model of the Hybrid Synchronous Machine

The mathematical model development of this machine will be based on the modeling of synchronous machine as contained in classical texts [18, 19]. In the analysis that follows, subscripts *abc* will be used to represent primary stator winding terms while subscripts *xyz* will be used to represent the secondary stator winding terms.

The voltage equations of the hybrid machine in machine variables are given in compact form as

$$V_H = I_H R_H + \frac{d\lambda_H}{dt} \tag{1}$$

where, V_H represents the (primary and secondary) stator and the rotor winding voltages and it is given in matrix form as:

$$V_H = \left[V_{abc}\, V_{xyz}\, V_{qdr} \right] = \left[V_a\, V_b\, V_c\, V_x\, V_y\, V_z\, V_{qr}\, V_{dr}\, V_{fr} \right] \tag{2}$$

The current matrix is given by

$$I_H = \left[I_{abc}\, I_{xyz}\, I_{qdr} \right] = \left[I_a\, I_b\, I_c\, I_x\, I_y\, I_z\, I_{qr}\, I_{dr}\, I_{fr} \right] \tag{3}$$

while the resistance matrix is

$$R_H = diag\left[R_a\, R_b\, R_c\, R_x\, R_y\, R_z\, R_{qr}\, R_{dr}\, R_{df} \right] \tag{4}$$

The flux linkages may be expressed compactly as

$$\lambda_H = \begin{bmatrix} \lambda_{abc} \\ \lambda_{xyz} \\ \lambda_{qdr} \end{bmatrix} = \begin{bmatrix} L_{11} & L_{12} & L_{13} \\ L_{21} & L_{22} & L_{23} \\ L_{31} & L_{32} & L_{33} \end{bmatrix} \begin{bmatrix} I_{abc} \\ I_{xyz} \\ I_{qdr} \end{bmatrix} = \begin{bmatrix} L_{abc} & L_{abcxyz} & L_{abcqdr} \\ L_{zxyabc} & L_{xyz} & L_{xyzqdr} \\ L_{qdrabc} & L_{qdrxyz} & L_{qdr} \end{bmatrix} \begin{bmatrix} I_{abc} \\ I_{xyz} \\ I_{qdr} \end{bmatrix} \tag{5}$$

From (5), L_{abc} is the sum of the 3×3 inductance matrix of the three-phase primary windings of both halves of the machine.

$$\therefore L_{abc} = L_{RR} + L_{SS} \tag{6}$$

where, L_{RR} is the inductance matrix of the round rotor half while L_{SS} is for the salient-pole half. The inductance matrix for the stator winding of any salient pole machine is well known in literature [18, 19] and it is given as

$$L_{ss} = \begin{bmatrix} L_{ls} + L_o - L_m \cos 2\theta_r & -\frac{1}{2}L_o - L_m \cos 2(\theta_r - \frac{\pi}{3}) & \cdots \\ -\frac{1}{2}L_o - L_m \cos 2(\theta_r - \frac{\pi}{3}) & L_{ls} + L_o - L_m \cos 2(\theta_r - \frac{2\pi}{3}) & \cdots \\ -\frac{1}{2}L_o - L_m \cos 2(\theta_r + \frac{\pi}{3}) & -\frac{1}{2}L_o - L_m \cos 2(\theta_r + \pi) & \cdots \\ & & \end{bmatrix}$$

$$\begin{matrix} & \\ & \\ -\frac{1}{2}L_o - L_m \cos 2(\theta_r + \frac{\pi}{3}) & \\ -\frac{1}{2}L_o - L_m \cos 2(\theta_r + \pi) & \\ L_{ls} + L_o - L_m \cos 2(\theta_r + \frac{2\pi}{3}) & \end{matrix} \tag{7}$$

where

$$L_o = \frac{1}{3}(L_{md} + L_{mq}) \quad \text{and} \quad L_m = \frac{1}{3}(L_{md} - L_{mq}) \tag{8}$$

In a round rotor machine, the air gap is uniform and so $L_{md} = L_{mq}$. From (8), $L_o = (2/3)L_{md}$ and $L_m = 0$, and the inductance matrix is thus reduced to:

$$\therefore L_{RR} = \begin{bmatrix} L_{ls} + \frac{2}{3}L_{md} & -\frac{1}{3}L_{md} & -\frac{1}{3}L_{md} \\ -\frac{1}{3}L_{md} & L_{ls} + \frac{2}{3}L_{md} & -\frac{1}{3}L_{md} \\ -\frac{1}{3}L_{md} & -\frac{1}{3}L_{md} & L_{ls} + \frac{2}{3}L_{md} \end{bmatrix} \tag{9}$$

$$\therefore L_{abc} = L_{SS} + L_{RR} =$$

$$\begin{bmatrix} 2L_{ls} + L_1 - L_m \cos 2\theta_r & -L_2 - L_m \cos 2(\theta_r - \frac{\pi}{3}) & \cdots \\ -L_2 - L_m \cos 2(\theta_r - \frac{\pi}{3}) & 2L_{ls} + L_1 - L_m \cos 2(\theta_r - \frac{2\pi}{3}) & \cdots \\ -L_2 - L_m \cos 2(\theta_r + \frac{\pi}{3}) & -L_2 - L_m \cos 2(\theta_r + \pi) & \cdots \\ & & \end{bmatrix}$$

$$\begin{matrix} & \\ & \\ -L_2 - L_m \cos 2(\theta_r + \frac{\pi}{3}) & \\ -L_2 - L_m \cos 2(\theta_r + \pi) & \\ 2L_{ls} + L_1 - L_m \cos 2(\theta_r + \frac{2\pi}{3}) & \end{matrix} \tag{10}$$

where,

$$L_1 = L_{md} + \frac{1}{3}L_{mq} \quad \text{and} \quad L_2 = \frac{1}{2}L_{md} + \frac{1}{6}L_{mq} \tag{11}$$

Also, L_{abcxyz} is the sum of the 3×3 inductance matrix as a result of the mutual inductance between the primary and the secondary stator windings of the machine.

On the assumption that the primary and secondary windings are identical, mutually coupled and occupy the same slot positions, the mutual inductance between the two sets of windings are equal, and each of them is equal to its self-inductance minus the leakage inductance [14].

Therefore, if, L_{MS} is the mutual inductance of the salient pole side; then, $L_{MS} = L_{SS} - L_l$. For the round rotor, $L_{MR} = L_{RR} - L_l$.

Since the secondary winding of the machine is transposed between the two halves, the mutual inductance between the primary and secondary

windings will be positive in one half of the machine and negative in the other half [14].

$$\therefore L_{abcxyz} = L_{RR} - L_l - (L_{SS} - L_l) = L_{RR} - L_{SS} =$$

$$\begin{bmatrix} L_3 + L_m\cos 2\theta_r & L_4 + L_m\cos 2(\theta_r - \frac{\pi}{3}) & \cdots \\ L_4 + L_m\cos 2(\theta_r - \frac{\pi}{3}) & L_3 + L_m\cos 2(\theta_r - \frac{2\pi}{3}) & \cdots \\ L_4 + L_m\cos 2(\theta_r + \frac{\pi}{3}) & L_4 + L_m\cos 2(\theta_r + \pi) & \cdots \end{bmatrix}$$

$$\begin{bmatrix} L_4 + L_m\cos 2(\theta_r + \frac{\pi}{3}) \\ -L_2 - L_m\cos 2(\theta_r + \pi) \\ L_3 + L_m\cos 2(\theta_r - \frac{2\pi}{3}) \end{bmatrix} \quad (12)$$

where,

$$L_3 = \frac{L_{md} - L_{mq}}{3} \quad \text{and} \quad L_4 = \frac{L_{mq} - L_{md}}{6} \quad (13)$$

Also, L_{abcqdr} is the sum of the mutual inductances between the primary stator and rotor windings of the two halves of the machine.

$$\therefore L_{abcqdr} = \left[L_{abcqdr}\right]_{RR} + \left[L_{abcqdr}\right]_{SS} =$$

$$\begin{bmatrix} (L_{md} + L_{mq})\cos\theta_r & 2L_{md}\sin\theta_r & \cdots \\ (L_{md} + L_{mq})\cos(\theta_r - \frac{2\pi}{3}) & 2L_{md}\sin(\theta_r - \frac{2\pi}{3}) & \cdots \\ (L_{md} + L_{mq})\cos(\theta_r + \frac{2\pi}{3}) & 2L_{md}\sin(\theta_r + \frac{2\pi}{3}) & \cdots \end{bmatrix}$$

$$\begin{bmatrix} 2L_{md}Sin\theta_r \\ 2L_{md}Sin(\theta_r - \frac{2\pi}{3}) \\ 2L_{md}Sin(\theta_r + \frac{2\pi}{3}) \end{bmatrix} \quad (14)$$

Since the primary and the secondary windings are identical and occupy the same slot position, then

$$\begin{cases} L_{xyzabc} = (L_{abcxyz})^T \\ L_{xyz} = L_{abc} \\ L_{qdrabc} = \left(L_{abcqdr}\right)^T \\ L_{qdrxyz} = \left(L_{xyzqdr}\right)^T \end{cases} \quad (15)$$

Due to the transposition of the secondary stator winding between the two-machine halves, the mutual inductance between the secondary winding and the rotor winding will be the algebraic sum of the mutual inductances of the two machine halves.

$$L_{xyzqdr} = \left[L_{xyzqdr}\right]_{RR} - \left[L_{xyzqdr}\right]_{SS}$$

$$= \begin{bmatrix} (L_{md} - L_{mq})\cos\theta_r & 0 & 0 \\ (L_{md} - L_{mq})\cos(\theta_r - \frac{2\pi}{3}) & 0 & 0 \\ (L_{md} - L_{mq})\cos(\theta_r + \frac{2\pi}{3}) & 0 & 0 \end{bmatrix} \quad (16)$$

Also, L_{qdr} is the self-inductance of the rotor winding of the hybrid machine and it is equal to the summation of self-inductance of the two machine halves. It is given as;

$$L_{qdr} = \left[L_{qdr}\right]_{RR} + \left[L_{qdr}\right]_{SS}$$

$$= \begin{bmatrix} L_{lq} + L_{mq} + L_{ld} + L_{md} & 0 & 0 \\ 0 & 2(L_{ld} + L_{md}) & 2L_{md} \\ 0 & 2L_{md} & 2(L_{lf} + L_{md}) \end{bmatrix} \quad (17)$$

It can be seen from (10), (12), and (14) that the inductance of the hybrid synchronous machine has some components that are rotor position-dependent and therefore, there is a need for transformation using the transformation matrix of (18) to get rid of the rotor position-dependent functions

$$T_{qdo}(\theta_r) = \frac{2}{3}\begin{bmatrix} \cos\theta_r & \cos(\theta_r - \frac{2\pi}{3}) & \cos(\theta_r + \frac{2\pi}{3}) \\ \sin\theta_r & \sin(\theta_r - \frac{2\pi}{3}) & \sin(\theta_r + \frac{2\pi}{3}) \\ \frac{1}{2} & \frac{1}{2} & \frac{1}{2} \end{bmatrix} \quad (18)$$

Therefore, applying (18) to (10), (12), and (14), the transformed flux linkage equations are given by

$$\begin{bmatrix} \lambda_{Qs} \\ \lambda_{qs} \\ \lambda_{qcg} \end{bmatrix} =$$

$$\begin{bmatrix} 2L_{ls} + L_{md} + L_{mq} & L_{md} - L_{mq} & L_{md} + L_{mq} \\ L_{md} - L_{mq} & 2L_{ls} + L_{md} + L_{mq} & L_{md} - L_{mq} \\ L_{md} + L_{mq} & L_{md} - L_{mq} & L_{ld} + L_{lq} + L_{md} + L_{mq} \end{bmatrix} \times$$

$$\begin{bmatrix} I_{Qs} \\ I_{qs} \\ I_{qcg} \end{bmatrix} \quad (19)$$

$$\begin{bmatrix} \lambda_{Ds} \\ \lambda_{ds} \\ \lambda_{dcg} \\ \lambda_{df} \end{bmatrix} =$$

$$\begin{bmatrix} 2(L_{ls} + L_{md}) & 0 & 2L_{md} & 2L_{md} \\ 0 & 2(L_{ls} + L_{md}) & 0 & 0 \\ 2L_{md} & 0 & 2(L_{ld} + L_{md}) & 2L_{md} \\ 2L_{md} & 0 & 2L_{md} & 2(L_{lf} + L_{md}) \end{bmatrix} \times$$

$$\begin{bmatrix} I_{Ds} \\ I_{ds} \\ I_{dcg} \\ I_{df} \end{bmatrix} \quad (20)$$

From (20), it is seen that the overall d-axis inductances are completely decoupled from the q-axis inductances whereas there are coupling terms between the d and q axes inductances in the overall q-axis inductance. This explains why the d-axis inductance is independent of the variation of the capacitor bank in the secondary winding.

It is worth noting that in this study, the primary and secondary windings have the same number of turns which implies unity turns ratio. Therefore, referring any of the machine parameters from secondary to primary or vice versa will retain the same value and consequently, referred parameters are not primed.

The voltage equations of this hybrid machine are given in (1) and when transformed to the rotor reference frame are given by

$$\begin{cases} V_{Qs} = 2r_s I_{Qs} + \omega_r \lambda_{Ds} + P\lambda_{Qs} \\ V_{Ds} = 2r_s I_{Ds} - \omega_r \lambda_{Qs} + P\lambda_{Ds} \end{cases} \quad (21)$$

$$\begin{cases} V_{qs} = 2r_s I_{qs} + \omega_r \lambda_{ds} + P\lambda_{qs} + V_{cq} \\ V_{ds} = 2r_s I_{ds} - \omega_r \lambda_{qs} + P\lambda_{ds} + V_{cd} \end{cases} \quad (22)$$

$$\begin{cases} V_{qcg} = 2r_{cg} I_{qcg} + P\lambda_{qcg} = 0 \\ V_{dcg} = 2r_{cg} I_{dcg} + P\lambda_{dcg} = 0 \\ V_{df} = 2r_f I_f + P\lambda_f \end{cases} \quad (23)$$

Equations (21)-(23) represent the primary, secondary and rotor windings respectively. It can be seen that the secondary stator winding has V_{cd} and V_{cq} components which account for the capacitor bank connected to it. They are given by Obe [12] in d-q as

$$\begin{cases} \dfrac{dV_{cd}}{dt} = \dfrac{i_d}{C} + \omega_r V_{cq} \\ \dfrac{dV_{cq}}{dt} = \dfrac{i_q}{C} - \omega_r V_{cd} \end{cases} \quad (24)$$

5 Steady-State Modeling of the Hybrid Machine

At steady-state, all the time-dependent components of (21)-(23) are set to zero and when (19) and (20) are substituted we have

$$\begin{cases} V_{Qs} = 2r_s I_{QS} + 2X_{DS} I_{DS} + 2E_i \\ V_{DS} = 2r_s I_{DS} - 2X_{QS} I_{QS} - X_{mr}(I_{QS} + I_{qs}) \\ V_{qs} = 2r_s I_{qs} + 2X_{ds} I_{ds} - X_c I_{ds} \\ V_{ds} = 2r_s I_{ds} - 2X_{qs} I_{qs} - X_{mr}(I_{Qs} + I_{qs}) + X_c I_{qs} \end{cases} \quad (25)$$

where, $E_i = X_{md} I_{df}$ [20] and $X_{mr} = (X_{md} – X_{mq})$.

The secondary stator winding of the machine is short-circuited, and therefore, $V_{qs} = V_{ds} = 0$. Also, since the primary and secondary stator windings of the machine are identical, their reactances are equal, ($\therefore X_{Ds} = X_{ds} = X_d$ and $X_{Qs} = X_{qs} = X_q$).

In a sinusoidal steady-state at synchronous speed, the following expressions hold [20];

$$\begin{cases} v_{ds} = -V_s \sin\delta \\ v_{qs} = \ V_s \cos\delta \end{cases} \quad (26)$$

where V_s is the supply voltage rms value and δ is the load angle.

When (26) is substituted into (25) and solving explicitly for I_{Ds}, I_{Qs}, I_{ds}, and I_{qs} gives

$$\begin{cases} I_{Ds} = \dfrac{V_s \cos\delta - 2E_i}{2X_d} \\ I_{Qs} = \dfrac{-(X_{mr} - X_c + 2X_q)V_s \sin\delta}{X_c X_{mr} + 2X_c X_q - 4X_q(X_{mr} + X_q)} \\ I_{ds} = 0 \\ I_{qs} = \dfrac{X_{mr} V_s \sin\delta}{X_c X_{mr} + 2X_c X_q - 4X_q(X_{mr} + X_q)} \end{cases} \quad (27)$$

For a typical double stator winding synchronous machine at steady-state, the following relationship exists between the two windings in rotor reference frame variables and synchronously rotating phasor [18]:

$$\begin{cases} F_1 = \left(F_{q1} - jF_{d1}\right)e^{j\delta} \\ F_2 = \left(F_{q2} - jF_{d2}\right)e^{j\delta} \end{cases} \quad (28)$$

where, F could be flux linkage, voltage or current phasors. If it is assumed that the q-axis is aligned to the phase A of the three-phase ABC system at this particular instant, the voltage input to the machine can be deduced from (25) to (28) and expressed as:

$$V_A = 2r_s I_A + j2X_d I_A + 2E_i + jX_{mr}(I_A + I_a) + U_1 \quad (29)$$

where, $U_1 = -\left(j2(X_d - X_q)I_{q1}e^{-j\delta} + X_{mr}(I_{d1}e^{-j\delta} + I_{d2}e^{-j\delta})\right)$.

$$V_a = 2r_s I_a + j2X_d I_a - jX_c I_a + jX_{mr}(I_A + I_a) + U_2 \quad (30)$$

where, $U_2 = -\left(j2(X_d + X_q)I_{q2}e^{-j\delta} - X_{mr}(I_{d1}e^{-j\delta} + I_{d2}e^{-j\delta})\right)$.

The per-phase steady-state equivalent circuit of the hybrid machine can be deduced from (29) and (30) and it is shown in Fig. 2.

5.1 Performance Characteristics of the Hybrid Machine

For the purpose of examining the performance of the hybrid machine, two identical 4-pole, 5kW, 220V, 50Hz, 3-phase line-start salient pole synchronous

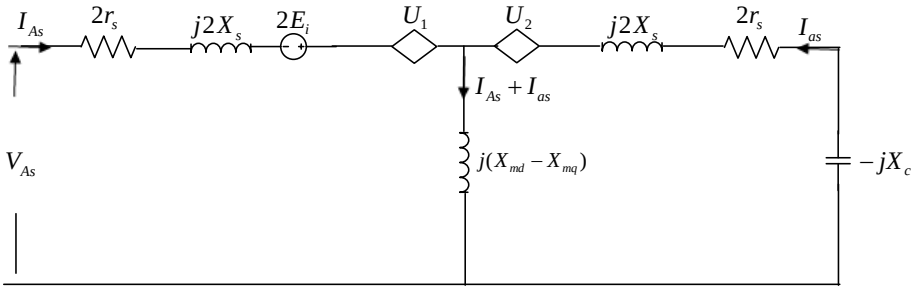

Fig. 2 Steady-state equivalent circuit of the hybrid machine.

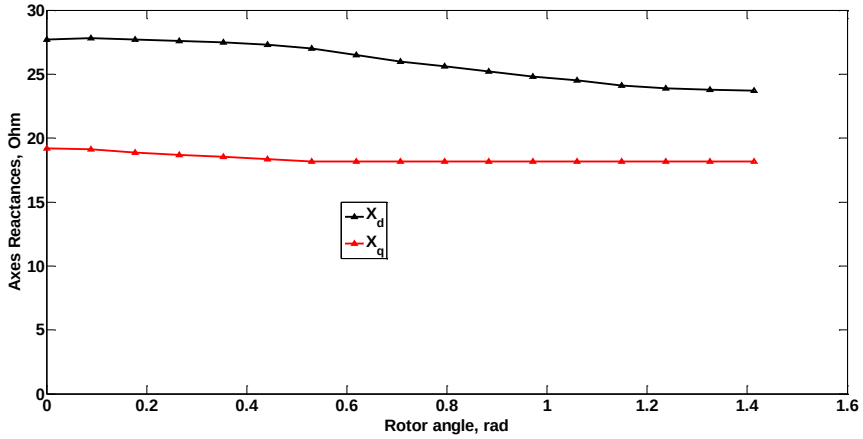

Fig. 3 Variation of axis reactances with load angle.

machines were acquired. The axial length of the machine is 85mm and the stator bore diameter is 92.5mm. The main air-gap length and the inter-polar slot air-gap are 0.4mm and 4mm respectively, while the pole-arc to pole-pitch ratio β is 0.65mm

The unsaturated reactances of the machine are: X_{md} = 26.512Ω, X_{mq} = 16.996Ω, X_{ls} = 1.194Ω, X_{lfr} = 94.248Ω, $X_{ldr} = X_{lqr}$ = 1.729Ω, while the resistances are r_s = 2.1Ω and r_{lfr} = 21Ω. The stator windings of both machines were split into two equal halves to form the primary and secondary windings respectively, thereby making the winding reactances one-quarter of its original value while the resistance will be half the original value. The salient rotor of the second half of the machine was discarded and now replaced with a fabricated round rotor with air-gap length g_0 of 0.39mm. The connection of the machine is as described in Section 2. Consequently, the parameters of the salient pole half of the hybrid machine now become: X_{md} = 6.628Ω, X_{mq} = 4.249Ω, X_{ls} = 0.2985Ω, X_{lfr} = 94.248Ω, $X_{ldr} = X_{lqr}$ = 1.729Ω, r_s = 1.05Ω and r_{lfr} = 21Ω.

In the steady-state analysis, an experimental variation [21, 22] of axes reactances X_d and X_q with load angle were determined. The quadrature axis reactance X_q was not affected by loading but the d-axis reactance was affected. These variations are shown in Fig. 3. To include the effect of saturation on the steady-state analysis, a third-degree polynomial curve-fit of the d-axis reactance was obtained as in (31) and used for the calculations at all values of change in load angle.

$$X_d = 4.1\delta^3 - 9.4\delta^2 + 2.4\delta + 28 \tag{31}$$

The synchronous reactance of the round rotor half X_s was made equal to the d-axis reactance of the salient-pole half X_d (i.e. $X_s = X_d$) by the adjustment of their air-gaps as described in [15] and given by

$$g_0 = \frac{1}{\left(\frac{1}{g_2}\right)+\left(\left(\frac{1}{g_1}\right)-\left(\frac{1}{g_2}\right)\right)\left(\beta+\frac{\sin\pi\beta}{\pi}\right)} \tag{32}$$

where, g_0 is the air-gap length of the round rotor half, g_1 and g_2 are the main air-gap length and inter-polar air-gap length respectively of the salient-pole half, while β is the pole arc to pole pitch ratio.

6 The Hybrid Machine Input Impedance

The input impedance of the hybrid machine can be obtained by finding the ratio of the input voltage V_{As} to the primary winding input current I_{As}.

$$Z_{in} = \frac{V_{As}}{I_{As}} \tag{33}$$

where, $V_{As} = V_{Qs} - jV_{Ds}$, and $I_{As} = I_{Qs} - jI_{Ds}$.

$$Z_{in} = \frac{V_{Qs} - jV_{Ds}}{I_{Qs} - jI_{Ds}} \tag{34}$$

Substituting (26) and (27) into (34) and simplifying gives:

$$Z_{in} = \frac{2X_d\left(X_cX_{mr} + 2X_cX_q + 4X_q\left(X_{mr} + X_q\right)\right)\left(\cos\delta + j\sin\delta\right)}{j\left(X_cX_{mr} + 2X_cX_q + 4X_q\left(X_{mr} + X_q\right)\right)\cos\delta + 2X_d\left(X_{mr} + 2X_q - X_c\right)\sin\delta} \tag{35}$$

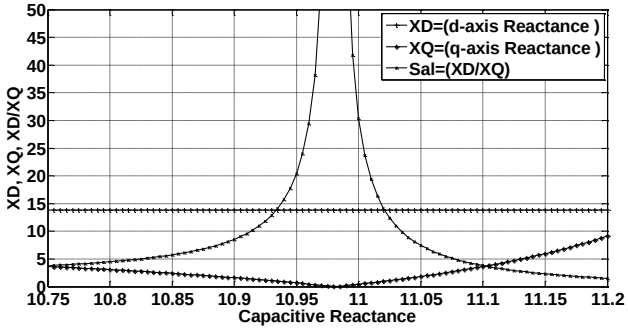

Fig. 4 Variation of the axes reactances and X_D/X_Q ratio with capacitive reactance.

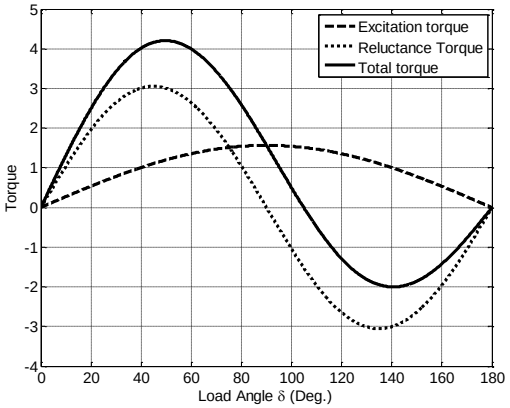

Fig. 5 The torque against load angle plot.

6.1 Axis Reactances of the Hybrid Machine

The input impedance of the hybrid machine of (35) can be resolved into two-axis components. The d-axis component will be referred to as the overall d-axis and will be represented as X_D, while the q-axis component will be referred to as the overall q-axis which will also be represented as X_Q.

6.2 Direct Axis Reactance

The overall direct axis reactance of the hybrid machine can be deduced by taking limit of $\delta \rightarrow 0$ in (35) and given by:

$$X_D = j2X_d \tag{36}$$

It can be seen from (36), that the d-axis reactance is independent of the capacitive reactance.

6.3 Quadrature Axis Reactance

As $\delta \rightarrow \pi/2$, the overall q-axis reactance is given by

$$X_Q = j\frac{4X_q\left(X_{mr} + X_q\right) - \left(X_{mr} + 2X_q\right)X_c}{X_{mr} + 2X_q - X_c} \tag{37}$$

It is evident in (37) that the overall quadrature axis reactance is dependent on the capacitance X_C of the capacitor that is connected in the secondary winding of the hybrid machine. Consequently, if the capacitive reactance is varied, only the overall q-axis reactance of the hybrid machine X_Q that will vary, without affecting the overall d-axis reactance X_D. It is thus possible to minimize X_Q without any deleterious effect on X_D.

It can be seen from (37) that the quadrature axis reactance is zero when;

$$X_c = \frac{4X_q\left(X_{mr} + X_q\right)}{2X_q + X_{mr}} \tag{38}$$

6.4 X_D/X_Q Reactance Ratio

The reactance ratio (X_D/X_Q) of the hybrid synchronous machine can be evaluated by taking the ratio of (36) and (37). The variation of X_D/X_Q with capacitive reactance X_C is shown in Fig. 4. It is seen that X_D is constant and independent of the capacitive reactance X_C while X_Q varies with the capacitive reactance X_C. At capacitive reactance X_C = 10.98Ω, which translates to 290 μF capacitor that X_Q = 0 and consequently, X_D/X_Q tends to infinity.

6.5 Steady-State Torque Equation

The expression for the electromagnetic torque of the hybrid machine is given by

$$T_e = \frac{3}{2}\frac{P}{2}\frac{1}{\omega_b}\left\{\left(\psi_{Ds}I_{Qs} - \psi_{Qs}I_{Ds}\right) + \left(\psi_{ds}I_{qs} - \psi_{qs}I_{ds}\right)\right\} \tag{39}$$

where the flux linkages are given as;

$$\begin{cases} \psi_{Qs} = 2X_{Qs}I_{Qs} + X_{mr}\left(I_{Qs} + I_{qs}\right) \\ \psi_{Ds} = 2X_{Ds}I_{Ds} + 2E_i \\ \psi_{qs} = 2X_{qs}I_{qs} + X_{mr}\left(I_{Qs} + I_{qs}\right) \\ \psi_{ds} = 2X_{ds}I_{ds} \end{cases} \tag{40}$$

Substituting (41) into (40) gives

$$\begin{aligned} T_e = \frac{3}{2}\frac{P}{2}\frac{1}{\omega_b}\Big[&\left(2X_{Ds}I_{Ds} + 2E_1\right)I_{Qs} \\ &-\left(2X_{Qs}I_{Qs} + X_{mr}\left(I_{Qs} + I_{qs}\right)\right)I_{Ds} + 2X_{ds}I_{ds}I_{qs} \\ &-\left(2X_{qs}I_{qs} + X_{mr}\left(I_{Qs} + I_{qs}\right)\right)I_{ds}\Big] \end{aligned} \tag{41}$$

Substituting the expression for currents (27) and simplifying gives

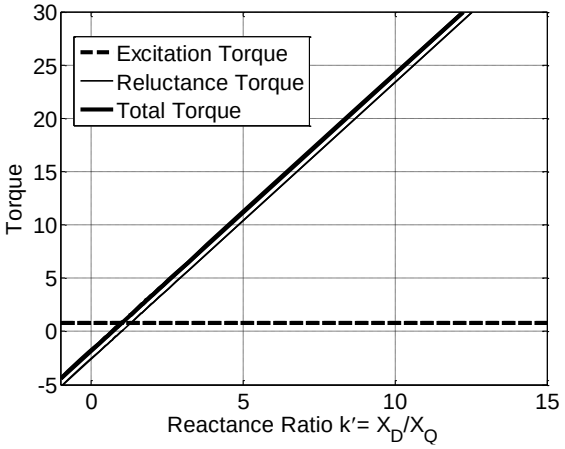

Fig. 6 Torque-reactance ratio plot.

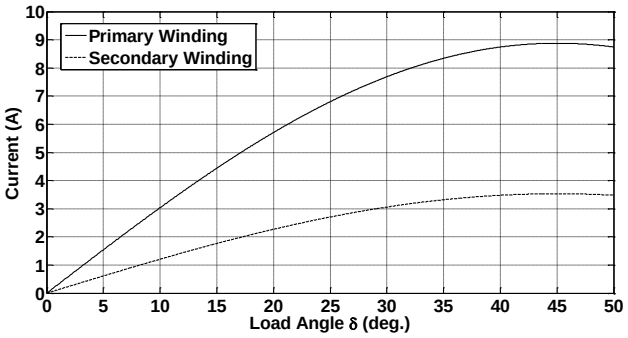

Fig. 7 Winding currents against load angle δ.

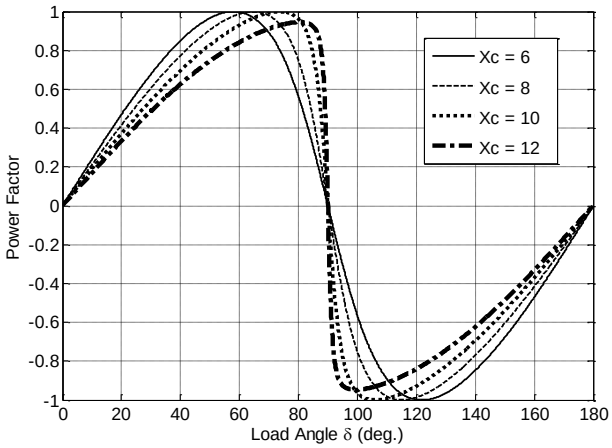

Fig. 8 Power factor-load angle plot.

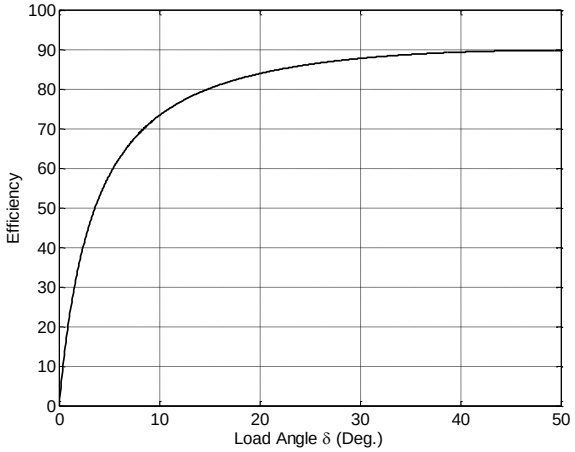

Fig. 9 Efficiency plot of the hybrid machine.

$$T_e = \frac{3}{2}\frac{P}{2}\frac{1}{\omega_b}\left(\frac{2E_iV_s\sin\delta}{X_D}+\left(\frac{k'-1}{2X_D}\right)V_s^2\sin 2\delta\right) \qquad (42)$$

where, $k' = X_D/X_Q$.

As can be seen from (42), just like the conventional synchronous machine, it is made up of the excitation and the reluctance torque components. Close examination of (42) shows that the excitation torque, which is the first component is independent of the quadrature axis reactance X_Q and hence capacitive reactance X_C. The reluctance torque, which is the second component is a function of the reactance ratio X_D/X_Q of the hybrid machine.

The plot of the torque against the load angle is as shown in Fig. 5.

Since the reactance ratio depends on the capacitive reactance at the secondary stator winding, then the reluctance torque is dependent on the capacitive reactance. The effect of the reactance ratio on the output torque of the hybrid machine can be seen in Fig. 6. It can be readily seen in Fig. 5 that at $X_D/X_Q = 3$ that the reluctance component of the output power is 2.5 times the excitation power

The primary winding current of the hybrid machine can be obtained from (33) while the secondary winding is obtained by applying current divider with respect to Fig. 2 and the plot of the currents against load angle is shown in Fig. 7.

7 The Power Factor of the Hybrid Synchronous Machine

The power factor of the hybrid machine could be obtained from the consideration of the machine input impedance and can be readily shown as:

$$\cos\varphi = \frac{R_e}{\sqrt{R_e^2 + X_e^2}} \qquad (43)$$

where, φ is the power factor angle, R_e is the real part of the input impedance, and X_e imaginary part of the input impedance.

The plot of the power factor against load angle for different values of the capacitive reactance X_C is shown in Fig. 8.

8 Efficiency of the Hybrid Machine

The efficiency of the machine is given as

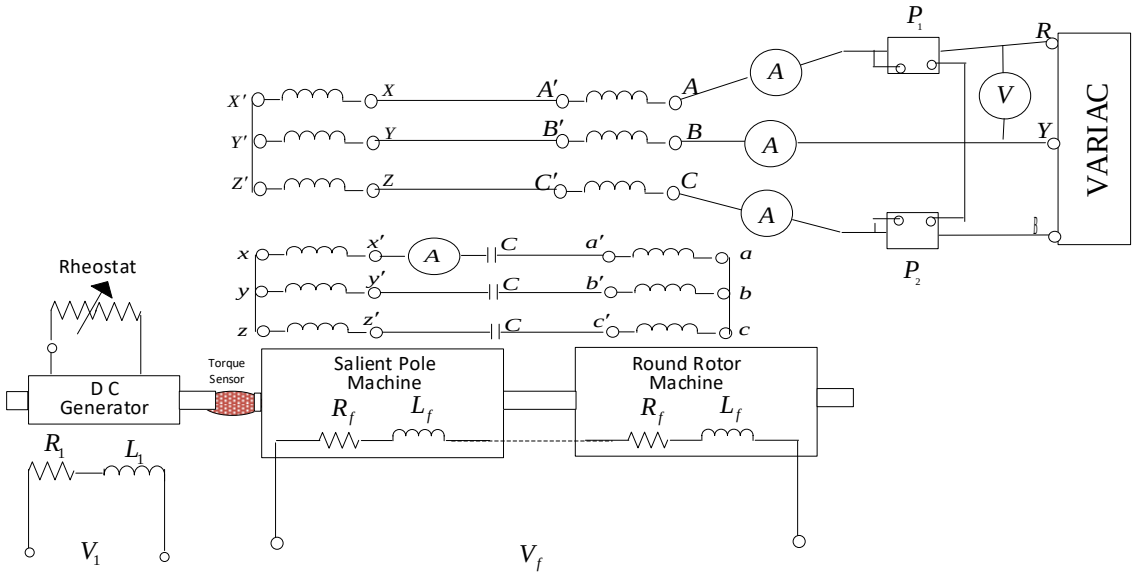

(a)

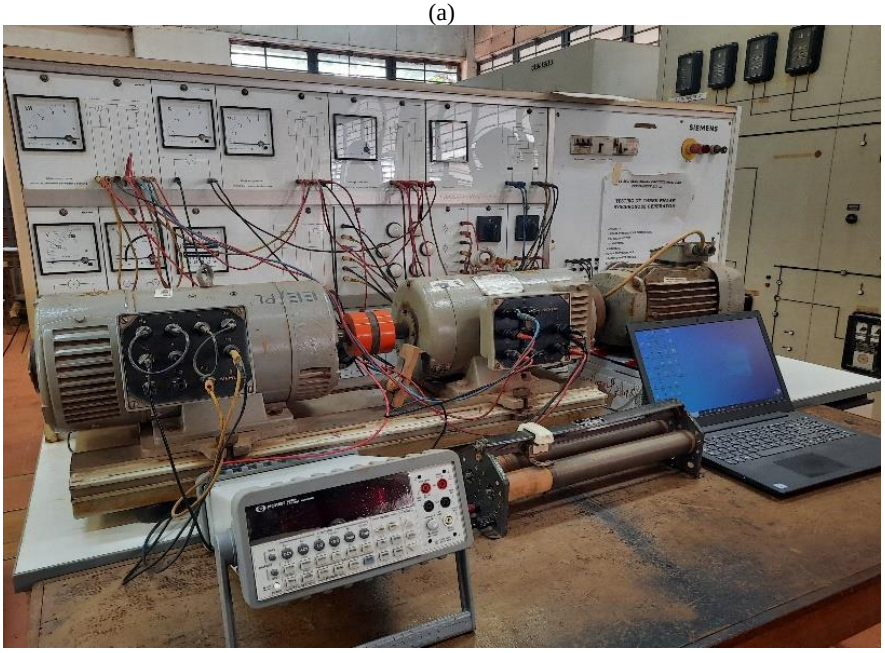

(b)

Fig. 10 The experimental setup of the hybrid machine; a) Connection diagram and b) Photograph.

$$\eta = \frac{P_{out}}{P_{in}} \times 100\% = \frac{P_{out}}{P_{loss} + P_{out}} \times 100\% \tag{44}$$

where, P_{out} is the output power of the machine and it can be gotten from (42) (i.e. $P = \omega_b T_e$), and P_{loss} is the I^2R losses in the windings, neglecting friction and windage. It is given as;

$$\begin{aligned} P_{loss} &= \frac{3}{2} r_s \left(i_{Ds}^2 + i_{Qs}^2 + i_{ds}^2 + i_{qs}^2 \right) + r_f' i_f'^2 \\ &= R_s \left(I_A^2 + I_a^2 \right) + I_f'^2 R_f' \\ &= 3 \times 2 \times R_s \left(I_A^2 + I_a^2 \right) + I_f'^2 R_f' \end{aligned} \tag{45}$$

The plot of the efficiency of the hybrid synchronous machine against load angle is as shown in Fig. 9

The efficiency of the hybrid machine is 89% which indicates much improvement from the conventional synchronous machine.

9 The Practical Machine

The description of the practical machine has been given in Section 5.1. The winding connection and the photograph of the hybrid machine are shown in Fig. 10.

The two machine elements were mechanically coupled together and then coupled to drive a dc generator feeding a variable resistance load through an RWT321 digital torque sensor. Two wattmeter method

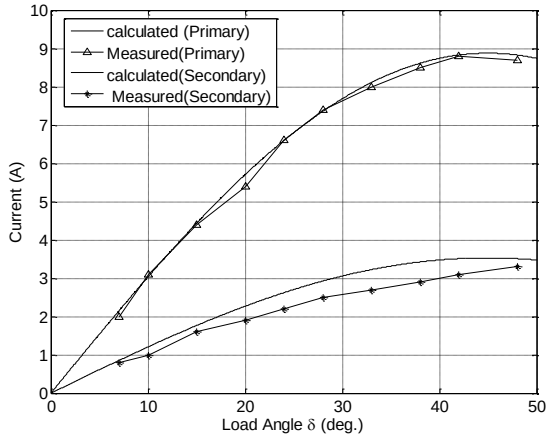

(a)

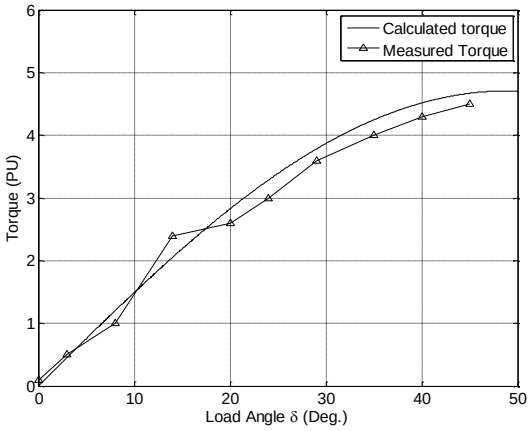

(b)

Fig. 11 a) Winding current and b) Torque.

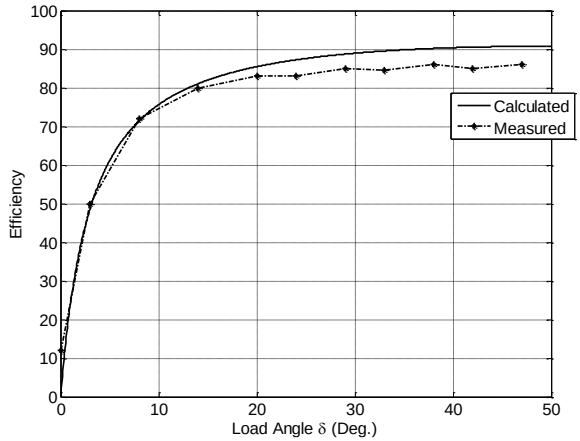

Fig. 12 Efficiency of the machine.

was used to measure the input power from which the power factor was calculated using $pf = \cos\left(\tan^{-1}\left(\sqrt{3}\frac{P_1 - P_2}{P_1 + P_2}\right)\right)$. The primary and secondary winding currents were measured with the variation of loads at a secondary winding capacitive reactance of 10.86Ω (which translates to 293μF) for optimal performance, while maintaining synchronous speed. The open-circuit and short-circuit tests were also carried out for determination of losses (hysteresis, eddy current, and copper losses). An open circuit was accomplished when the capacitors were removed from the secondary winding and their terminals left open, the primary winding being the only one in operation. The short circuit test was realized when the capacitors were inserted and tuned to the value for minimum impedance which in this case was 290μF. The winding currents and the torque were measured and their plots in comparison with the calculated values are shown in Fig. 11. The efficiency is as shown in Fig. 12.

10 Conclusions

A new hybrid synchronous machine is modeled and the steady-state performance analysis is carried out. At X_D/X_Q = 3, the reluctance component of the output power is 2.5 times the excitation component. As the X_D/X_Q ratio is further increased by the capacitor tuning, the reluctance component of the output power increases proportionally up to the steady-state stability limit, which can be made much greater than the excitation power.

The machine is quite suitable for bulk power generation because of the inherent high output capability which could be optimized for wind power generation because of the ease of adjusting the output power to compensate for variation in wind speed.

It is observed that the maximum output power of the hybrid machine occurs very close to the load angle of a salient-pole synchronous machine operating in the pure synchronous reluctance mode. This is because the reluctance component of the output power is much higher than the field excitation component, and hence dominates the behavior of the machine.

Intellectual Property

The authors confirm that they have given due consideration to the protection of intellectual property associated with this work and that there are no impediments to publication, including the timing of publication, with respect to intellectual property.

Acknowledgment

The authors are grateful to the management of Scientific Equipment Development Institute (SEDI), Akwuke-Enugu, Nigeria for machining the rotors used for this study to their designed shapes and sizes, and to the Alexander von Humboldt Foundation of Bonn, Germany for donating most of the measuring instruments used in the experiments.

CRediT Authorship Contribution Statement

E. O. Agbachi: Conceptualization, Methodology,

Software, Formal analysis, Writing - Original draft. **L. U. Anih:** Supervision. **E. S. Obe:** Data curation.

Declaration of Competing Interest

The authors hereby confirm that the submitted manuscript is an original work and has not been published so far, is not under consideration for publication by any other journal and will not be submitted to any other journal until the decision will be made by this journal. All authors have approved the manuscript and agree with its submission to "Iranian Journal of Electrical and Electronic Engineering".

References

[1] P. J. Lawrenson and L. A. Agu, "Theory and performance of polyphase reluctance machines," *Proceedings of the Institution of Electrical Engineers*, Vol. 111, No. 8, p. 1435, 1964.

[2] T. A. Lipo, "Synchronous reluctance machines-a viable alternative for ac drives?," *Electric Machines and Power Systems*, Vol. 19, No. 6, pp. 659–671, 1991.

[3] N. G. Ozcelik, U. E. Dogru, M. Imeryuz, and L. T. Ergene, "Synchronous reluctance motor vs. Induction motor at low-power industrial applications: Design and comparison," *Energies*, Vol. 12, No. 11, pp. 1–20, 2019.

[4] S. Cai, M. J. Jin, and H. H. and J. X. Shen, "Comparative study on synchronous reluctance and PM machines," *COMPEL: The International Journal for Computation and Mathematics in Electrical and Electronic Engineering*, Vol. 35, No. 2, pp. 607–623, 2016.

[5] S. M. De Pancorbo, G. Ugalde, J. Poza, and A. Egea, "Comparative study between induction motor and Synchronous Reluctance Motor for electrical railway traction applications," in *IEEE 5th International Electric Drives Production Conference (EDPC)*, pp. 2–6, 2015.

[6] D. A. Staton, T. J. E. Miller, and S. E. Wood, "Maximising the saliency ratio of the synchronous reluctance motor," in *IEE Proceedings B: Electric Power Applications*, Vol. 140, No. 4, pp. 249–259, 1993.

[7] J. Rizk, M. H. Nagrial, and A. Hellany, "Optimum design parameters for synchronous reluctance motors," in *Proceedings of the 14th International Middle East Power Systems Conference (MEPCON'10)*, Cairo University, Egypt, pp. 813–818, 2010.

[8] S. Yammine, C. Henaux, M. Fadel, S. Desharnais, and L. Calégari, "Synchronous reluctance machine flux barrier design based on the flux line patterns in a solid rotor," in *International Conference on Electrical Machines (ICEM 2014)*, pp. 297–302, 2014.

[9] L. U. Anih and L. A. Agu, "A novel strategy for raising the unit output of large synchrnous machine," *Nigerian Journal of Technology*, Vol. 22, No. 1, pp. 24–28, 2003.

[10] E. S. Obe and T. Senjyu, "Analysis of a polyphase synchronous reluctance motor with two identical stator windings," *Electric Power Systems Research*, Vol. 76, pp. 515–524, 2006.

[11] A. S. O. Ogunjuyigbe, A. A. Jimoh, D. V. Nicolae, and E. S. Obe, "Analysis of synchronous reluctance machine with magnetically coupled three-phase windings and reactive power compensation," *IET Electric Power Applications*, Vol. 4, No. 4, p. 291, 2010.

[12] E. S. Obe, "Steady-state performance of a line-start synchronous reluctance motor with capacitive assistance," *Electric Power Systems Research*, Vol. 80, No. 10, pp. 1240–1246, 2010.

[13] L. U. Anih and E. S. Obe, "Performance analysis of a composite dual-winding reluctance machine," *Energy Conversion and Management*, Vol. 50, pp. 3056–3062, 2009.

[14] L. U. Anih, E. S. Obe, and S. E. Abonyi, "Modelling and performance of a hybrid synchronous reluctance machine with adjustable Xd/Xq ratio," *IET Electric Power Applications*, Vol. 9, No. 2, pp. 171–182, 2015.

[15] E. S. Obe, "Small signal analysis of load-angle governing and excitation control of AC generator," *Nigerian Journal of Technology*, Vol. 24, No. 2, pp. 19–33, 2005.

[16] M. I. Enwelum and E. O. Agbachi, "Hybrid synchronous machine capable of high output power for optimizing the potentials in Nigeria's extractive industries," *International Journal of Research in Engineering & Advanced Technology*, Vol. 2, No. 6, pp. 109–126, 2015.

[17] S. E. Abonyi, "Performance of a hybrid synchronous reluctance machine capable of ultra-high output power," *Unpublished Ph.D. Thesis*, Department of Electrical Engineering. University of Nigeria, Nsukka, Nsukka, 2016.

[18] P. C. Krause, W. Oleg, and S. D. Scott, *Analysis of electric machinery and drive systems*. John Wiley & Sons, 2013.

[19] C. M. Ong, *Dynamic simulation of electric machinery using MATLAB/Simulink*. New Jersey: Prentice-Hall PTR, 1998.

[20] T. A. Lipo, *Analysis of synchronous machines*. Boca Raton: Taylor & Francis Group, 2012.

[21] T. W. Nehl, F. A. Fouad, and N. A. Demerdash, "Determination of saturated values of rotating machinery incremental and apparent inductances by an energy perturbation method," *IEEE Transactions on Power Apparatus and Systems*, No. 12, pp. 4441–4451, 1982.

[22] E. S. Obe, "Measurement of transient and steady-state load angle in synchronous machines," *Unpublished Masters of Engineering Thesis*, University of Nigeria, Nsukka, 1999.

E. O. Agbachi received his B.Eng. degree, Electrical and Computer Engineering in 2004 and M.Eng. degree, Electrical Engineering in 2010 from the Federal University of Technology Minna, Nigeria, and University of Nigeria, respectively. He is currently studying for his Ph.D. degree in the Department of Electrical Engineering of the University of Nigeria Nsukka. He is also a lecturer in the Department of Electrical and Electronics Engineering, Federal University of Technology, Minna.

L. U. Anih was born on September 23, 1959. He received B.Eng. degree in 1984, M.Eng. degree in 1988, and Ph.D. degree in 1999, all in Electrical Engineering from Anambra State University of Science and Technology Enugu, Obafemi Awolowo University Ile- Ife and University of Nigeria, Nsukka (UNN) respectively. He has been teaching at the university since 1989 and rose to the rank of Professor in 2009. He was the head of the Department of Electrical Engineering, University of Nigeria, Nsukka from 2000-2003; Director, Computer Communications Centre (UNN) from 2012-2014; Director, Students Industrial Works Experience Scheme from 2011-2017. He is a member of the Nigeria Society of Engineers (NSE), a Member of the Council for the Regulation of Engineering in Nigeria (COREN), and a member of IEEE. His research interest is in dual stator winding synchronous machines and has been published widely in reputable journals.

E. S. Obe received his B.Eng., M.Eng., and Ph.D. degrees in Electrical Engineering from University of Nigeria in 1994, 1999, and 2002, respectively. Since 1999 he has been with the Department of Electrical Engineering, University of Nigeria, Nsukka where he is currently a Professor. Prof. Obe has been a visiting researcher at Tennessee Technological University, the USA in 2004 and 2006, at the University of the Ryukyus, Japan in 2005, and Technische Universitat Darmstadt, Germany 2008-2009. He has held several key positions at the University of Nigeria including Director, National Center for Equipment Maintenance and Development, (2012-2014), Director, Computer Communications Center (2014-2018), Coordinator, International Interventions Programs (2016-2019), Head of Electrical Engineering Department, UNN (2016-2019), Associate Dean, Faculty of Engineering (2018-2020). In August 2020, Prof. Obe was elected Dean, Faculty of Engineering, University of Nigeria, a position he currently occupies. Prof. Obe is an Associate Editor of IET Electric Power Applications of UK, Associate Editor of Electric Power Components and Systems, and Editor-in-Chief, Nigerian Journal of Technology. He is a fellow of AvH, Germany, Fellow of Matsumae International Foundation of Japan, Member IEEE, Member NSE, and a registered corporate engineer in Nigeria. His research interests are ac machine analysis, design and drives. Prof. Obe has published over 50 articles in reputable journals and high echelon conference proceedings.